Effect of strain-rate and material characteristics on the seismic residual capacity of reinforced concrete plastic hinges: numerical investigation

A. Cuevas & S. Pampanin

Department of Civil Engineering, University of Canterbury, Christchurch.

2015 NZSEE Conference

ABSTRACT: According to capacity design principles, structures are designed to withstand major earthquakes by developing inelastic action and energy dissipation in concentrated regions referred to as plastic hinges. Thus, when using traditional monolithic connections, structural damage is expected to occur in the form of well distributed cracks along the plastic hinge region. Observations from previous earthquakes have shown, however, that under some circumstances a single crack opening can occur, concentrating all the plastic strain at a single location and potentially leading to premature fracture of the reinforcing steel after a few high-amplitude cycles.

This paper presents a qualitative framework of an ongoing research project aiming at investigating the seismic residual capacity or "life" of reinforced concrete frames. Preliminary results of numerical parametric investigations on a well-designed reinforced concrete beam-column joint is presented, in order to investigate and understand, both qualitatively and quantitatively, the effects on the cracking pattern of parameters such as strain-rate, steel and concrete material properties, as well as the amount of longitudinal reinforcement.

It was (preliminary) observed that less cracks with wider crack openings are expected to occur for smaller yielding strength for the steel, f_y , and larger longitudinal reinforcement ratio, ρ_s (when compared to the minimum threshold as from NZS 3101:2006), values. Moreover, it was observed that the tensile strength of the concrete, f_t, strongly affects the expected cracking pattern in the beam-column joints, the latter being more uniform (i.e., more cracks with narrower crack openings) for lower values. In the cyclic response the secant stiffness and hysteretic damping tend to become stable after a few cycles. More investigation is under development to ascertain the above statements.

1 INTRODUCTION

According to capacity design principles developed since the 1960s-1970s, structures are designed to withstand major earthquakes by developing inelastic action and energy dissipation in concentrated regions referred to as plastic hinges. This in turn, and almost inevitably when using traditional monolithic connections, leads to structural damage, often over the irreparability threshold. The aftermath of the Christchurch earthquakes sequence in 2010-2011 has highlighted the crucial need to move towards a damage control philosophy and low-damage technologies whilst improving assessment and repairing techniques for more traditionally designed plastic hinges (Pampanin, 2012).

Despite the availability and recent development of seismic assessment and rehabilitation guidelines, they are mainly focused to the evaluation of the vulnerability and improvement of the seismic performance of existing buildings designed prior to capacity design principles. Essentially, residual capacity of buildings has been traditionally assessed by means of empirical modification factors mostly calibrated on experimental observations (e.g., Maeda et al, 2004; Polese et al., 2012; FEMA 306). Depending on the amount of damage observed after the earthquake account for residual drifts,

stiffness and strength reductions of those damaged elements. Very little information and assistance is provided in assessing the residual capacity of damaged buildings, even those relatively well designed according to modern seismic codes. This lack of understanding and knowledge on the residual capacity of reinforced concrete structures, in terms of number and intensity of aftershocks the structure could withstand following a major earthquake and during its remainder life-time has led, in the aftermath of the Canterbury earthquake, to an unprecedented extensive number of post-earthquake demolitions of modern buildings. The above is especially important when assessing existing, yet well designed buildings, where (and depending on the amount and type of observed damage) the risk of collapse during an aftershock (or a series of) might not be apparent if the assessment is performed based only on stiffness and strength degradation.

When considering the problem of residual capacity of typical plastic hinges within the context of residual fatigue life, past research has tended to primarily focus on bridge columns (Kunnath et al., 1997; Mander and Cheng, 1999), and specifically on the assessment of the low-cycle fatigue of the longitudinal reinforcement (Mander et al., 1994; Abdalla et al., 2009; Haliweh et al., 2010), often based on the assumption that the failure in a reinforced concrete element can be attributed to either the low-cycle fatigue of the longitudinal reinforcing steel, the failure of the concrete due to either lack of confinement or the fracture of the transverse hoop reinforcement, and/or the buckling of the longitudinal reinforcement in compression. The latter two mechanisms can be easily avoided if sufficient transverse reinforcement is provided (Mander and Cheng, 1999). However, as it has been observed after recent earthquakes, the low cycle fatigue of the longitudinal reinforcement is only one part of the overall picture; there are other factors such as bond deterioration between steel and concrete, the amount of longitudinal and transverse reinforcement, as well as the characteristics of steel and concrete materials that strongly influences the plastic hinge behaviour, its cracking pattern and therefore, its overall residual capacity.

This paper presents a (qualitative) framework of the ongoing numerical and analytical investigation aiming at investigating the residual fatigue life of reinforced concrete frames at a component (or plastic hinge) level. Results of an experimental and numerical investigation on a modern (i.e., relatively well-designed according to post-1970s seismic codes) reinforced concrete beam-to-column joint are also discussed, targeting at identifying and understanding, both qualitatively and quantitatively, the effects of parameters such as bond deterioration, steel and concrete material properties, rate of loading, as well as the amount of longitudinal reinforcement, on the cracking pattern and on the nonlinear behaviour of reinforced concrete plastic hinges.

2 ACCOUNTING FOR RESIDUAL CAPACITY OF REINFORCED CONCRETE PLASTIC HINGES

2.1 New framework to account for residual capacity in seismic design and assessment processes

A new framework to account for residual capacity at a plastic hinge level was first proposed in Cuevas and Pampanin (2014), alongside its implementation within a full displacement-based approach for the design and assessment processes of multi-degree-of-freedom systems.

As shown in Figure 1, the framework comprises four main steps. The first two are related to current practice adapted for this purpose; while the other two refers to past research that is revisited, modified and complemented with new research based on the current knowledge, new evidences and latest available tools. Herein, the first component (Figure 1a) is related to seismic demand, where the elastic spectrum for the design or assessment approach is defined either as code-based or as a response spectrum from actual records (for post-earthquake evaluations and required earthquake interventions).

The second component (Figure 1b) is related to the estimation of the equivalent number of cycles the structure will experience during the mainshock, $n_{D,1}$ (and at a later stage, during the aftershocks, $n_{D,2}$ etc). This low-cycle fatigue demand of reinforced concrete structures might be assessed through fatigue demand spectra generated from spectral results of inelastic SDOF systems as proposed by Mander and Cheng (1999), and more recently by Mander and Rodgers (2013).

The third step (Figure 1c) is related to the evaluation of the plastic drifts,$\theta_{p,1}$ and fatigue life relationships, referred to as the amount of cycles the plastic hinge can sustain during the mainshock, N_1, (and eventually, during the aftershocks, N_2 etc) before failure occurs, whereas the fourth and final step (Figure 1d) in the proposed framework is related to the estimation of the remaining residual capacity of the plastic hinge to resist aftershocks, expressed as a ratio between the fatigue life (N_2) and the cyclic demand ($n_{D,1}$), once a big portion of its initial capacity has been consumed during a mainshock. More detailed information on this qualitative framework can be found in Cuevas et al. (2014).

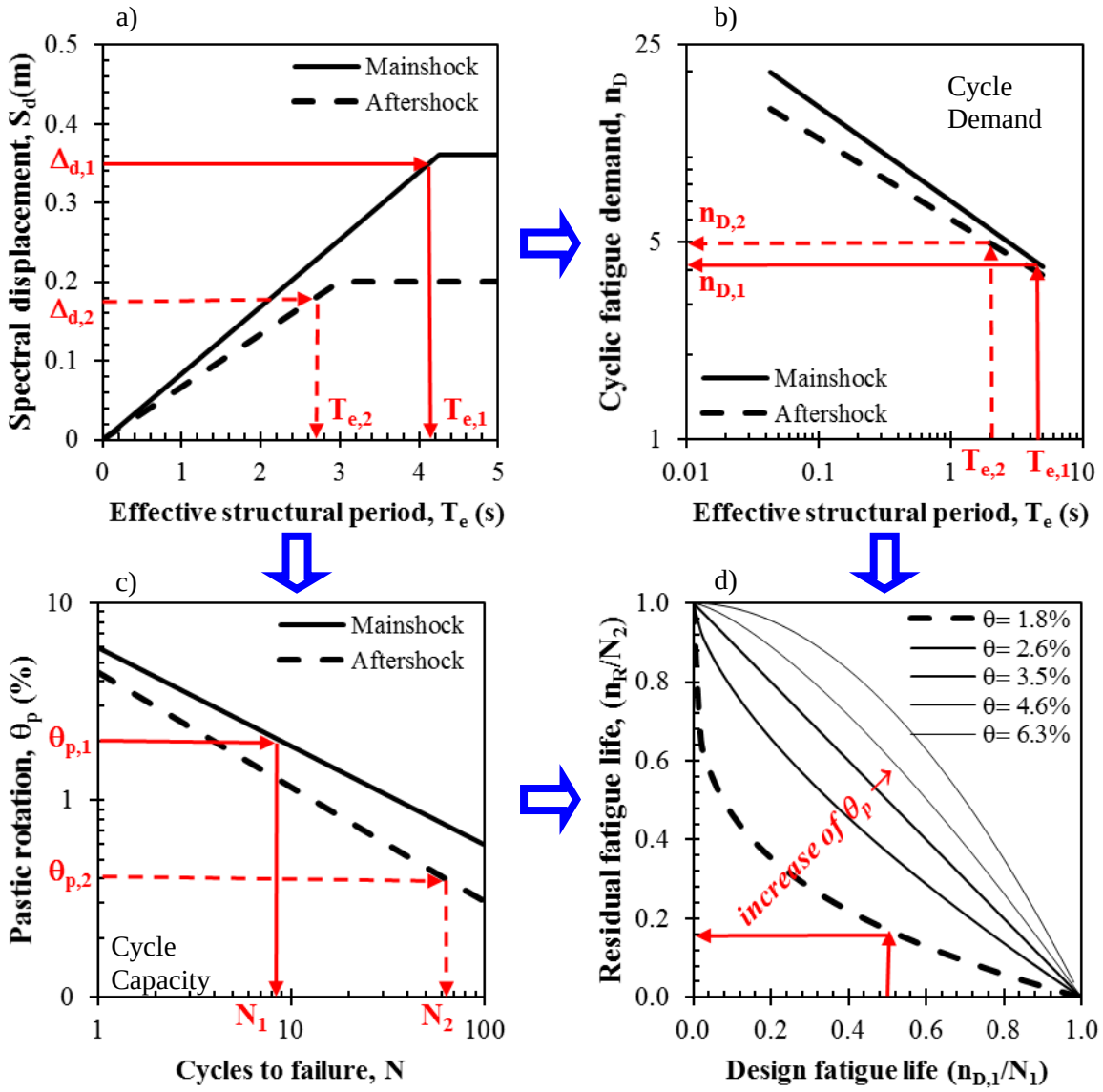

Figure 1. Main components of the new residual capacity model (Cuevas and Pampanin, 2014).

After the 2010-2011 Canterbury earthquake sequence, in a number of cases few major cracks opening were observed instead of a well distributed cracking pattern expected in those plastic hinge locations were plastic deformation was expected to occur, causing a large amount of deformation concentrated at a single location and leading to a low-cycle fatigue of the reinforcing steel (SESOC, 2011). Therefore, as stated in Cuevas and Pampanin (2014), in order to provide reliable estimates of the residual capacity of a plastic hinge region, it is necessary, to address the main issues of how such plastic strains and fatigue life relationships are affected by factors such as rate of loading, bond deterioration, longitudinal reinforcement ratios, as well as material characteristics (e.g., strain hardening of steel, concrete tensile strengths).

Aiming at investigating the effect of the above observations, analytical and numerical investigations (and experimental tests at a later stage) are under development as part of this research program. In the following, a qualitative framework of the ongoing research to fully address the issues of plastic strain and fatigue life relationships (Figure 1c and Figure 1d) is described.

2.2 **Qualitative framework to assess the residual fatigue life of plastic hinges**

Figure 2 shows the main suggested steps to assess the residual fatigue life of a reinforced concrete plastic hinge. The qualitative framework can be explained as follows. For a given (well-designed following capacity design principles) beam-column joint (Figure 2a, exterior and interior), a series of monotonic Finite Element (FE) simulations are performed, and the strain at the most critical location in the plastic hinge is monitored so that a relationship between plastic strain and drift demand is obtained (see Figure 2b). Parametric analyses changing the steel and concrete material properties, amount of reinforcement and rate of loading will be performed, aiming at identifying different cracking patterns and their influence in the plastic strain and residual fatigue life of the plastic hinge.

Once the effect of such factors have been identified, cyclic FE simulations will be performed and the variation of plastic strain (and plastic strain energy) cycle after cycle (due to bond deterioration and damage in the plastic hinge region) will be investigated. Figure 2c schematically exemplifies the above, where a beam-column joint has been subjected to several equi-amplitude (drift based) cycles.

The third step involved in the process deals with the estimation of relationships between the number of cycles the plastic hinge can resist before reaching either low-cycle fatigue or buckling of the reinforcing steel (Figure 2d). For that purpose, information available in literature is being calibrated. For instance, Mendes and Castro (2014) developed a new constitutive model for the simulation of reinforcing steel bars, including a model to account for ultra-low-cycle fatigue effects by simply multiplying the yield surfaces by a fatigue factor γ_f, which depends on cumulative plastic strain and some other factors controlling the fatigue evolution.

Once such relationships have been obtained, the number of cycles N_1 and N_2 required to reach failure due to either low-cycle fatigue or buckling of the reinforcing steel can be obtained by tracking the plastic strain (and plastic strain energy) evolution up to failure (see Figure 2e).

The above steps will be used to account for residual fatigue life in both design of new plastic hinges as well as assessment of existing ones, whereas the following two steps are more assessment related.

Firstly, relationships between the maximum crack width and strain at the most critical location will be investigated by monotonic FE analyses (see Figure 2f). It has been observed during experimental investigations that the strains "measured" (since the real measurement is hardness) with non-destructive testing (NDTs) does not change regardless the number of cycles the specimen has been subjected to (Giuseppe Loporcaro, personal communication), therefore the maximum expected crack width during a single (monotonic) push for the same "measured" strain can be estimated with such relationships.

Secondly, cyclic FE analyses will be performed in order to investigate the increase of crack width (compared with the monotonic case) due to cyclic demand. Thus, for a given strain at the most critical location (estimated with NDTs), the equivalent number of cycles the plastic hinge has been subjected to can be estimated Figure 2g).

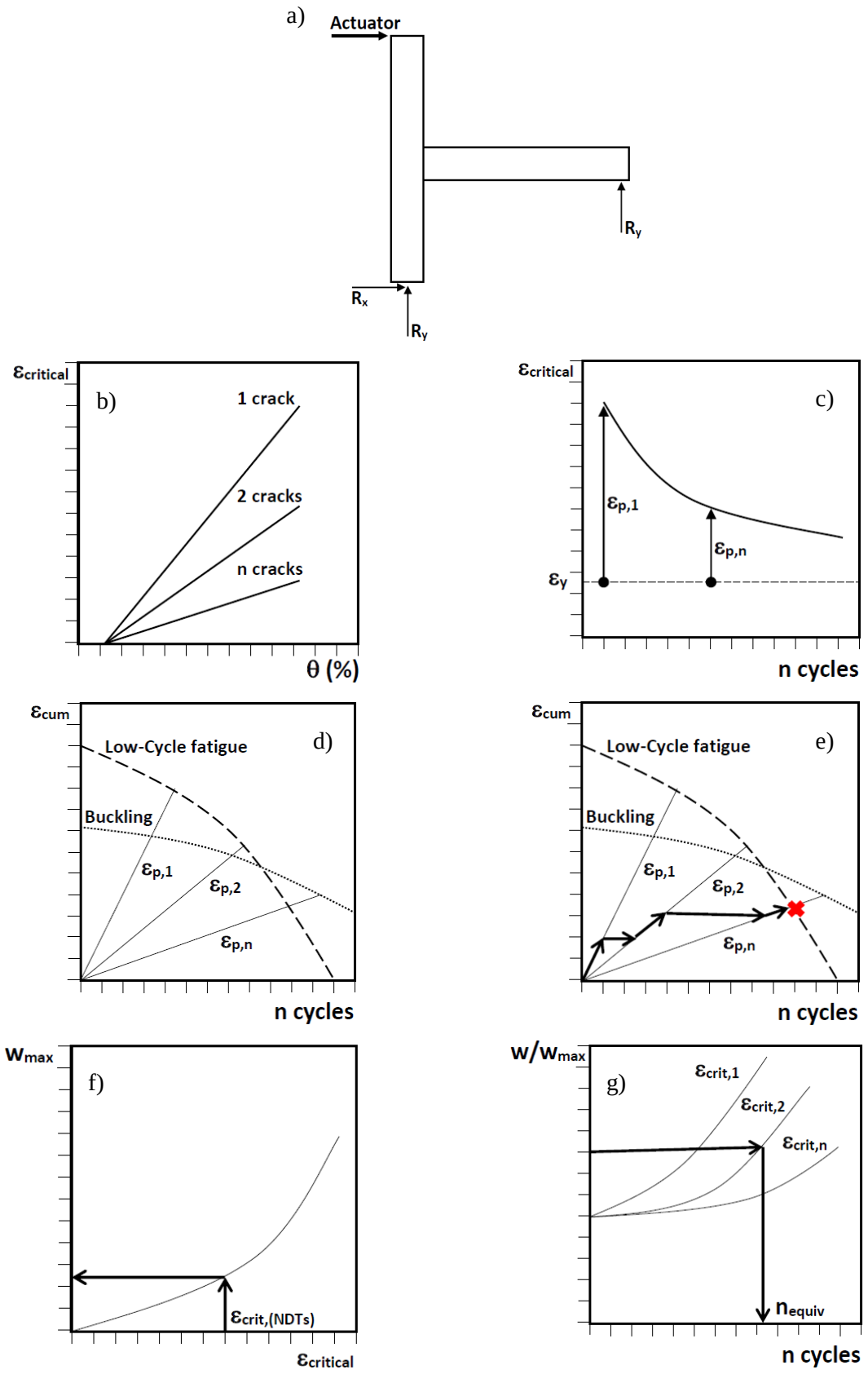

Figure 2. Main suggested steps to evaluate the residual fatigue life of a reinforced concrete plastic hinge

3 NUMERICAL INVESTIGATION: PRELIMINARY RESULTS

Analytical and numerical investigations are under development in order to calibrate the aforementioned (qualitative) framework. Some of the (preliminary) results are briefly outlined in this section. The nonlinear FE code MASA developed at the Institute for Construction Materials (IWB) of the University of Stuttgart (Ožbolt et al., 2001), was used in this study. In this code the concrete is modelled according to a microplane model, consisting of a three-dimensional (3D) microscopic model in which the material is characterized by uniaxial relations between the stress and strain components on planes of various orientations called "microplanes". The smeared-crack concept was used for the modelling of the cracking of the concrete, and the reinforcing bars were represented with one-dimensional (1D) truss elements with a three-linear constitutive law.

The bond between the longitudinal reinforcement and concrete was modelled using discrete bond elements consisting of 1D nonlinear springs (see Figure 3), whereas for transverse reinforcement a rigid connection between steel and concrete was assumed, neglecting the influence of the relative displacement between the stirrups and the concrete (Eligehausen et al., 2009). This discrete bond model is able to predict the bond behaviour of deformed bars under monotonic and cyclic loading; the bond deterioration is assumed to occur after some slip due to mechanical damage in the concrete-to-steel interface surrounding the ribs (Eligehausen et al., 1983; Lettow, 2006).

Hexahedral elements with side lengths of approximately 15mm in the joint area and the plastic hinge regions, as well as 50mm elsewhere were used to create the mesh of the elements. Linear elastic elements were used at the vicinities of the supports and the point of load application so that local failure of concrete elements due to excessive stresses is avoided. Mirror symmetry (i.e., symmetry about a vertical plane across a mid-section in the beam-column joint) was used to drastically reduce the total amount of nodes and elements and thus the required computational time.

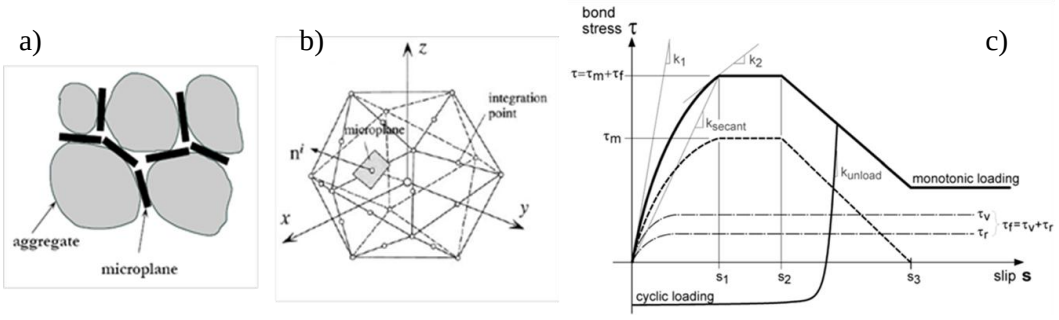

Figure 3. Microplane model: a) load transfer over a number of idealized contact planes; b) spatial discretization of unit-volume sphere by 21 microplanes (Ozbolt et al., 2001); c) Discrete bond model as implemented in MASA (Lettow, 2006).

Prior to perform parametric analyses the FE model has been validated with the experimental results of a beam-column joint designed according to the latest concrete code in NZ (NZS3101:2006, under review and amendments following the 2010-2011 earthquakes sequence) to achieve a weak-beam and strong-column hierarchy (see Figure 4). More detailed information about the validation, testing protocol and specimen characteristics can be found in Cuevas et al. (2014). In the following, different limit states have been defined as proposed by Priestley et al. (2007). For normal structures, Level 1 (Serviceability Limit State, SLS) refers to a 50% probability of exceedance in 50 years intensity level; Level 2 (Damage-control Limit State, DLS) to a 10% probability of exceedance in 50 years intensity level; and Level 3 (Ultimate Limit State, ULS) to a 2% probability of exceedance in 50 years.

3.1 Influence of concrete and steel strength, f'_c, f_y, and reinforcement ratio, ρ_s

Figure 5 shows the results of the same specimen with two different concrete compressive strength (and thus tensile strength and bond characteristics). While with f'_c of 20MPa two wide cracks are being developed, one single crack is developed with f'_c of 40MPa and consequently the plastic strain at the most critical location is increased.

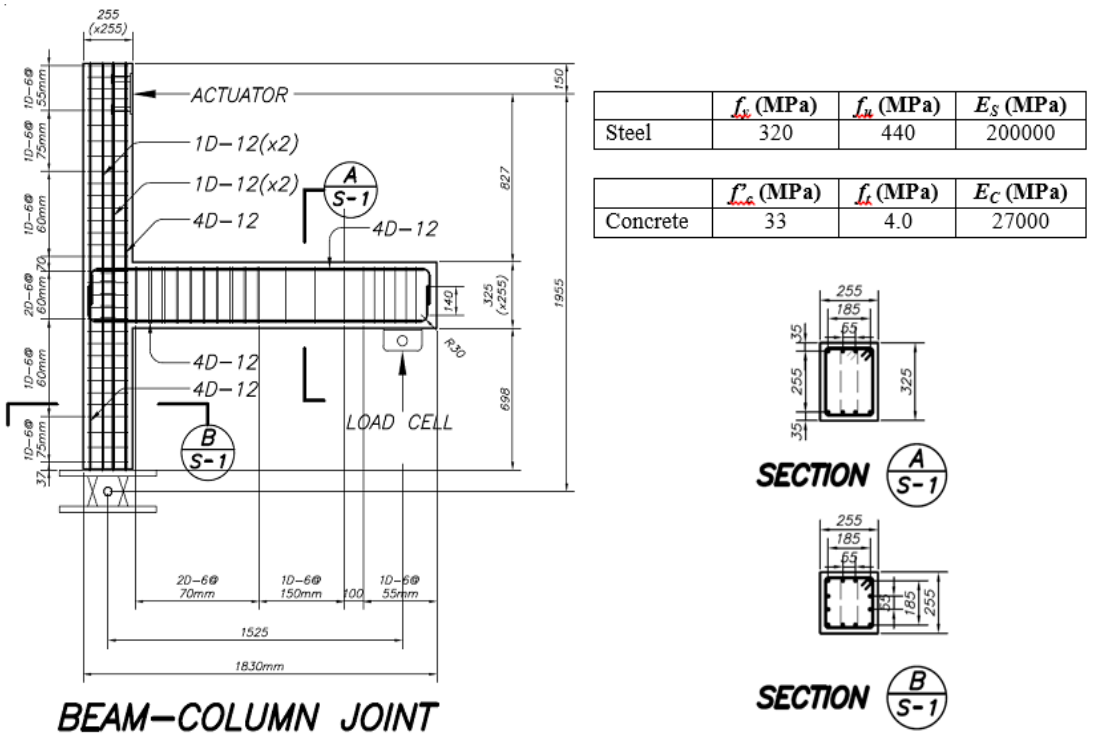

	f_y (MPa)	f_u (MPa)	E_S (MPa)
Steel	320	440	200000

	f'_c (MPa)	f_t (MPa)	E_C (MPa)
Concrete	33	4.0	27000

Figure 4. Experimental setup of the two-thirds scale specimen and material characteristics.

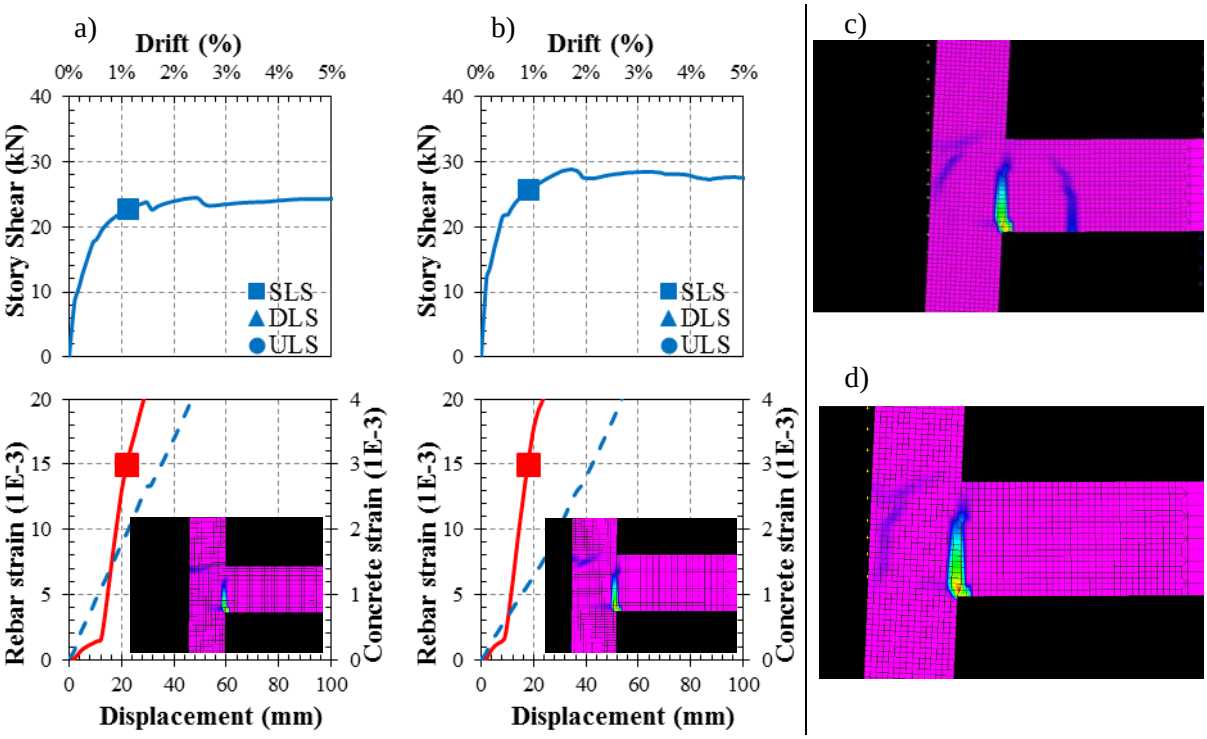

Figure 5. Monotonic story shear vs displacement response from the numerical results; and steel and concrete strains for simulations: a) f'_c 20MPa, f_y 300MPa and ρ_s 0.61% (BCJ-2); b) f'_c 40MPa, f_y 300MPa and ρ_s 0.61% (BCJ-6) (the dashed-line represents concrete strains, whereas the solid line represent the rebar strain; the small snapshot represent the cracking pattern at SLS). Snapshots for c) BCJ-2 and d) BCJ-6 at DLS. The solid square represents the Serviceability Limit State (SLS); the solid triangle the Damage-control Limit State (DLS), and the solid circle the Ultimate Limit State (ULS), not observed here.

It was also observed that the cracking pattern is not affected when the reinforcement ratio was increased from 0.61% to 1.09% by keeping unchanged the concrete strength; two major cracks were observed in both cases (see Figure 6). Interestingly enough (and as expected) a single major crack was observed for lower reinforcement ratios when the concrete strength (in both cases) is increased to 40MPa (see Figure 7).

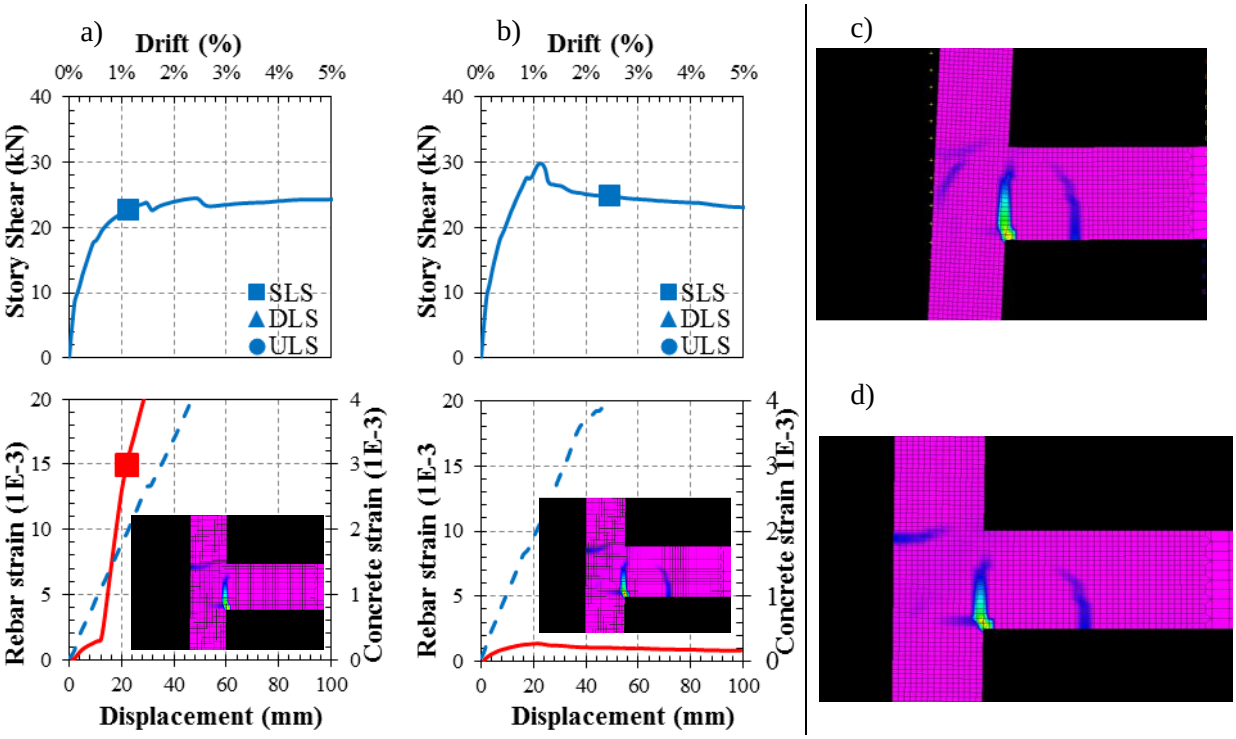

Figure 6. Monotonic story shear vs displacement response from the numerical results; and steel and concrete strains for simulations: a) f'_c 20MPa, f_y 300MPa and ρ_s 0.61% (BCJ-2); b) f'_c 20MPa, f_y 300MPa and ρ_s 1.09% (BCJ-3) (the dashed-line represents concrete strains, whereas the solid line represent the rebar strain; the small snapshot represent the cracking pattern at SLS). Snapshots for c) BCJ-2 at DLS and d) BCJ-3 at drift equivalent to DLS of BCJ-2. The solid square represents the Serviceability Limit State (SLS); the solid triangle the Damage-control Limit State (DLS), and the solid circle the Ultimate Limit State (ULS), not observed here.

Table 1 shows the material characteristics as well as the reinforcement ratios and minimum reinforcement content (ρ_{min}, as per NZS 3101:2006, clause 9.3.8.2.1) for each of the simulations. It is interesting to note that (as per code) multiple cracks are expected to occur since the longitudinal reinforcement content is above the minimum required, however, large plastic deformations at few locations (one-to-two major cracks) were observed in the simulations.

Table 1. Material characteristics and reinforcement ratios for simulations BCJ-2, BCJ-3, BCJ-6 and BCJ-7 (ρ_{min} as per NZS 3101:2006, and the tensile strength of concrete estimated as $f_t = 0.8\sqrt{f'_c}$).

Simulation	f_y (MPa)	f'_c (MPa)	$\sqrt{f'_c}$ (MPa)	f_t (MPa)	ρ_s (%)	ρ_{min} (%)
BCJ-2	300	20	4.5	3.6	0.61	0.37
BCJ-3	300	20	4.5	3.6	1.09	0.37
BCJ-6	300	40	6.3	5.0	0.61	0.53
BCJ-7	300	40	6.3	5.0	1.09	0.53

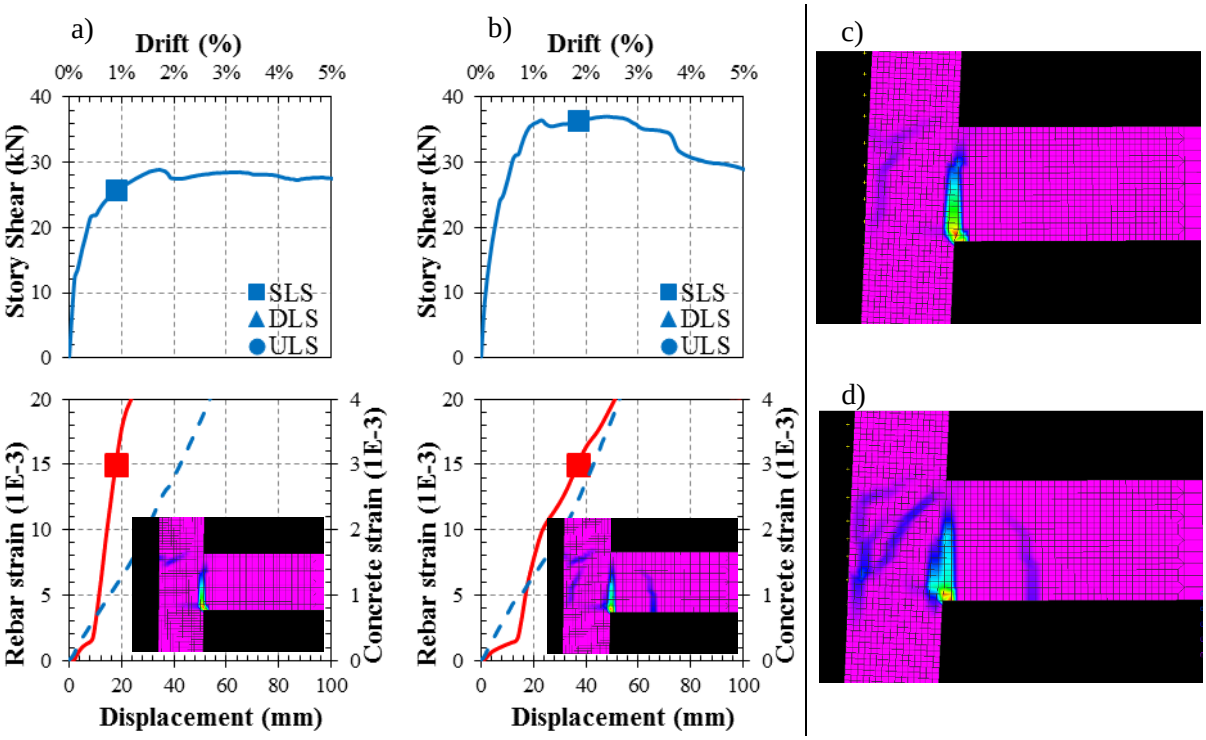

Figure 7. Monotonic story shear vs displacement response from the numerical results; and steel and concrete strains for simulations: a) f'_c 40MPa, f_y 300MPa and ρ_s 0.61% (BCJ-6); b) f'_c 40MPa, f_y 300MPa and ρ_s 1.09% (BCJ-7) (the dashed-line represents concrete strains, whereas the solid line represent the rebar strain; the small snapshot represent the cracking pattern at SLS). Snapshots for c) BCJ-6 at DLS and d) BCJ-7 at drift equivalent to DLS of BCJ-2. The solid square represents the Serviceability Limit State (SLS); the solid triangle the Damage-control Limit State (DLS), and the solid circle the Ultimate Limit State (ULS), not observed here.

3.2 Influence of f_t on the cracking pattern and limit states

In Figure 5 it was observed that variations on f'_c affect the expected cracking pattern in the beam-column joints. Since the unconfined compressive concrete strength has a strong impact on the tensile concrete strength, three additional simulations with f_t of 2MPa, 3.5MPa and 5MPa, representing realistic values for f'_c of 30-to-35MPa (assuming an upper characteristic modulus of rupture of $\sqrt{f'_c}$; Henry, 2013), were adopted by keeping unchanged the other parameters.

As seen in Figure 8, although the overall behaviour of the three simulations is comparable in terms of strength, stiffness and strain limits, the cracking pattern is strongly affected by the tensile strength of concrete f_t, being more uniform (i.e., larger amount and less intense cracks) for lower values, and more concentrated in one single crack for higher values. This latter behaviour is consistent with the observations occurred in the aftermath of the Canterbury earthquakes sequence and confirms the primary role that the tensile strength of concrete, for other constant parameters, can have in the cracking pattern and thus residual capacity of structural components and connections.

More detailed information regarding this (preliminary) parametric analysis can be obtained in Cuevas et al. (2014)

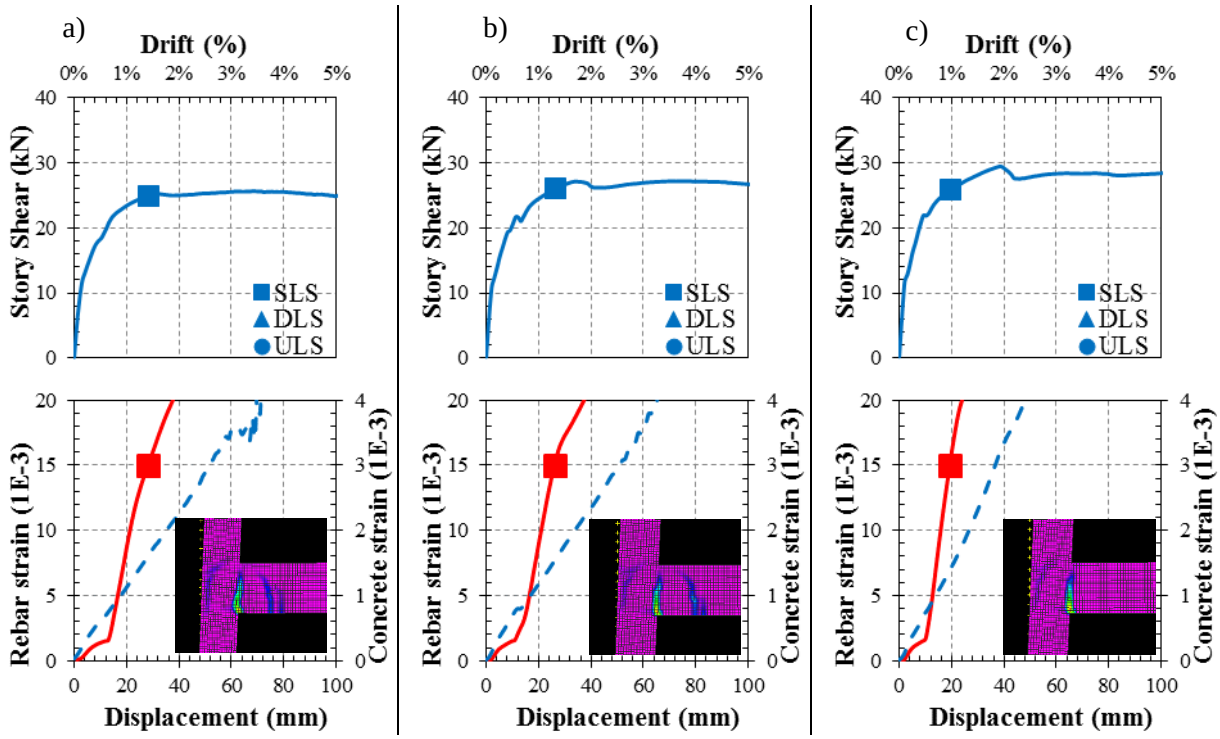

Figure 8. Monotonic story shear vs displacement response from the numerical results; and steel and concrete strains for simulations: a) f_t 2MPa; b) f_t 3.5MPa; c) f_t 5MPa (the dashed-line represents concrete strains, whereas the solid line represent the rebar strain; the small snapshot represent the cracking pattern at DLS). The solid square represents the Serviceability Limit State (SLS). For all simulations, f'_c of 33MPa, f_y of 320MPa and ρ_s of 0.61% were used.

3.3 Rate of loading and cyclic response of the specimen

The same model was further modified in order to make it more compatible with what was observed during the test, specifically the technique in which the hook within the joint is modelled has been improved. After this modification, FE analyses with different rates of loading were performed (see Ozbolt and Sharma, 2011; and Ozbolt et al, 2011, for theory and applications of MASA under dynamic loads), and as can be seen in Figure 9, no evident difference on the cracking pattern, strength and stiffness is observed, apart from a localised strain concentration migrating towards the plastic hinge at higher rates of loading. These results although preliminary are in agreement with those from Chung and Shah (1989); they observed that beam-column joints tested at high rate of loading with a relatively large amount of shear reinforcement (typical for well-detailed beam-column joints) maintained load carrying capacities similar to those tested at low rate of loading.

Different rates of loading were also applied for different tensile concrete strengths. As can be seen from Figure 10, (preliminary) strain rate effects are not as critical for high strain concentrations due to single crack openings as it is the tensile concrete strength.

Similarly, different rates of loading were applied for different reinforcement ratios (ρ_s varying from 0.43% to 1.09%). From Figure 11 it is evident that strain rate effects do not (preliminary) influence on the cracking pattern for different reinforcement content. However, small variations in the cracking pattern were observed for low reinforcement content as it approaches to the minimum required as per NZS 3101:2006 (ρ_{min} = 0.45%).

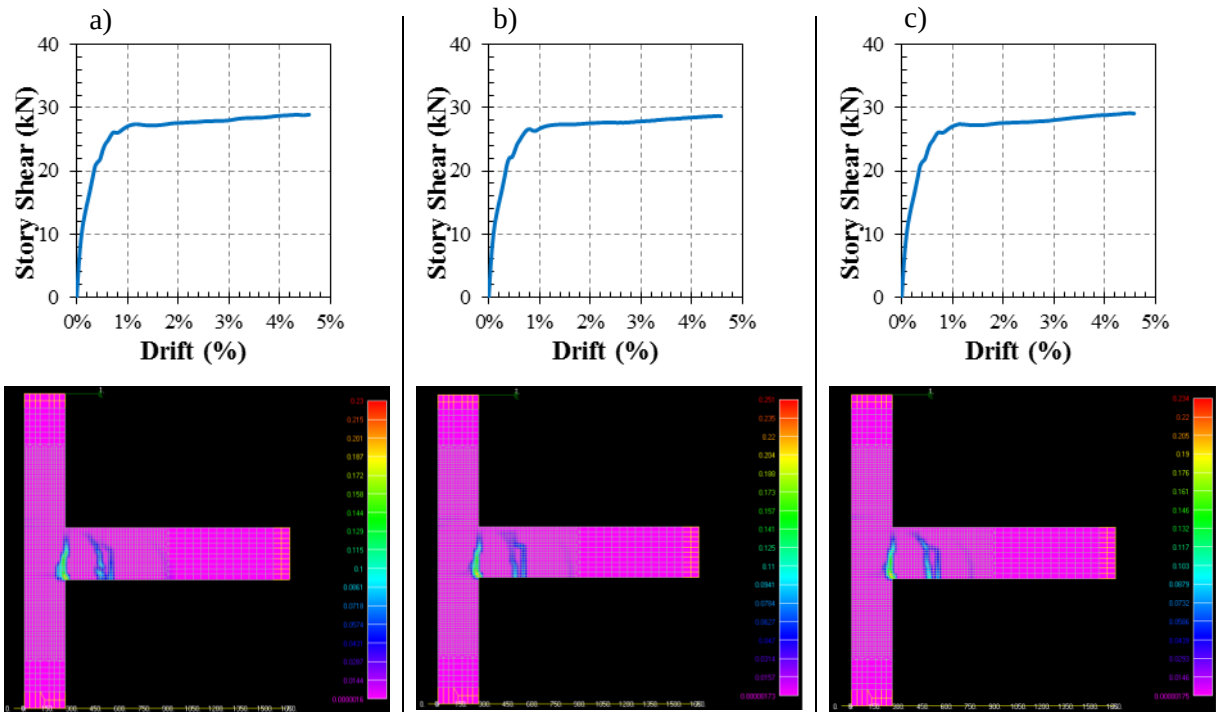

Figure 9. Monotonic story shear vs displacement response and snapshots from the numerical results: a) pseudo-static case; b) rate of loading of 10cm/s; and c) rate of loading of 100cm/s. For all simulations, f'_c of 33MPa, f_y of 320MPa and ρ_s of 0.61% were used.

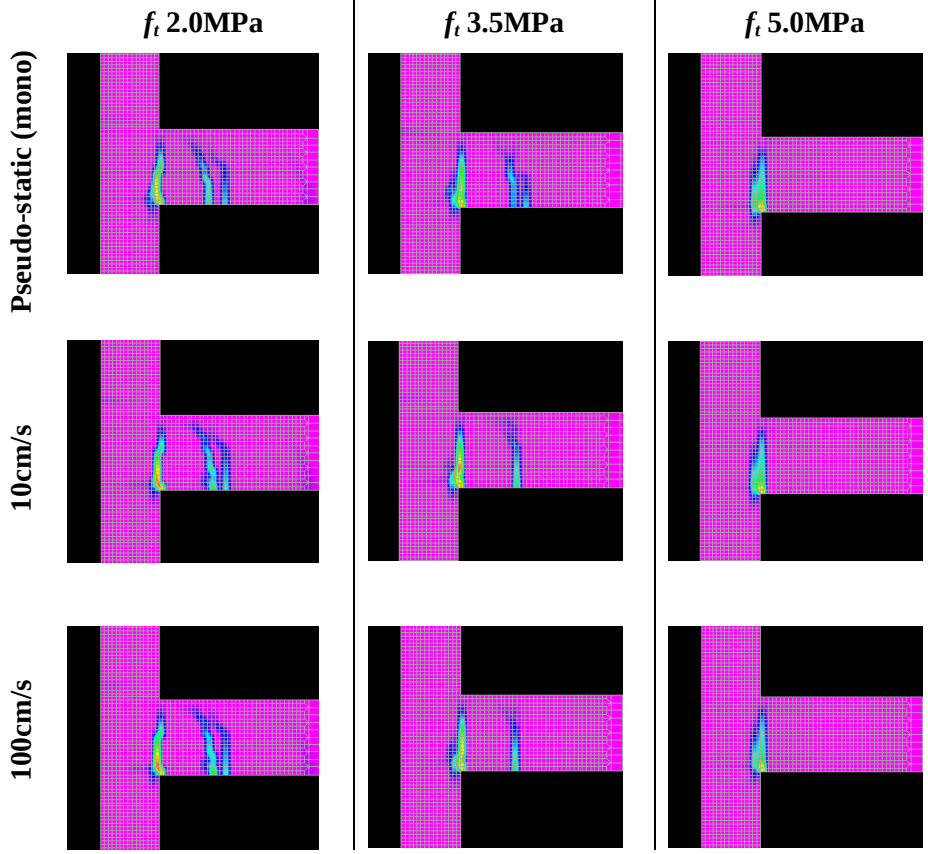

Figure 10. Screenshots from FE analyses varying the concrete tensile strength and rate of loading. For all simulations, f'_c of 33MPa, f_y of 320MPa and ρ_s of 0.61% were used.

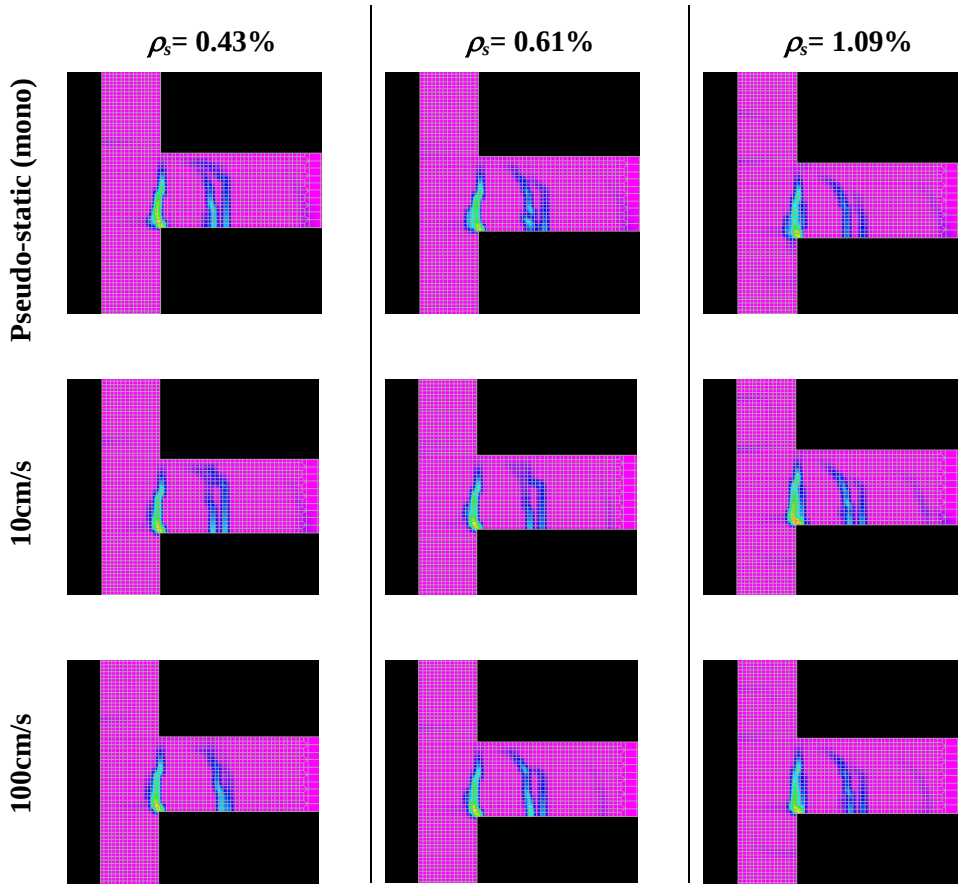

Figure 11. Screenshots from FE analyses varying the longitudinal reinforcement content and rate of loading. For all simulations, f'_c of 33MPa and f_y of 320MPa were used.

Figure 12 shows the variation of steel strain and neutral axis depth with the applied displacement for the same FE simulations as shown in Figure 11. It is evident how the strain rate effect is more critical for low reinforcement ratios. More so, the figure shows similar results for rates of loading of 10cm/s and 100cm/s, differentiating between those from static (mono) and dynamic load.

In addition, a preliminary cyclic analysis was also performed by applying six (pseudo-static) cycles of 1.5% drift, for different reinforcement content. Figure 13 shows the preliminary results. It is evident how the maximum strain decreases cycle after cycle (due to damage in the concrete and bond deterioration). More so, it is interesting to note how the secant stiffness and hysteretic damping decrease considerably in the first cycle(s) but then becomes almost unchanged for further cycles, an important feature to bear in mind when accounting for residual capacity in design and assessment processes.

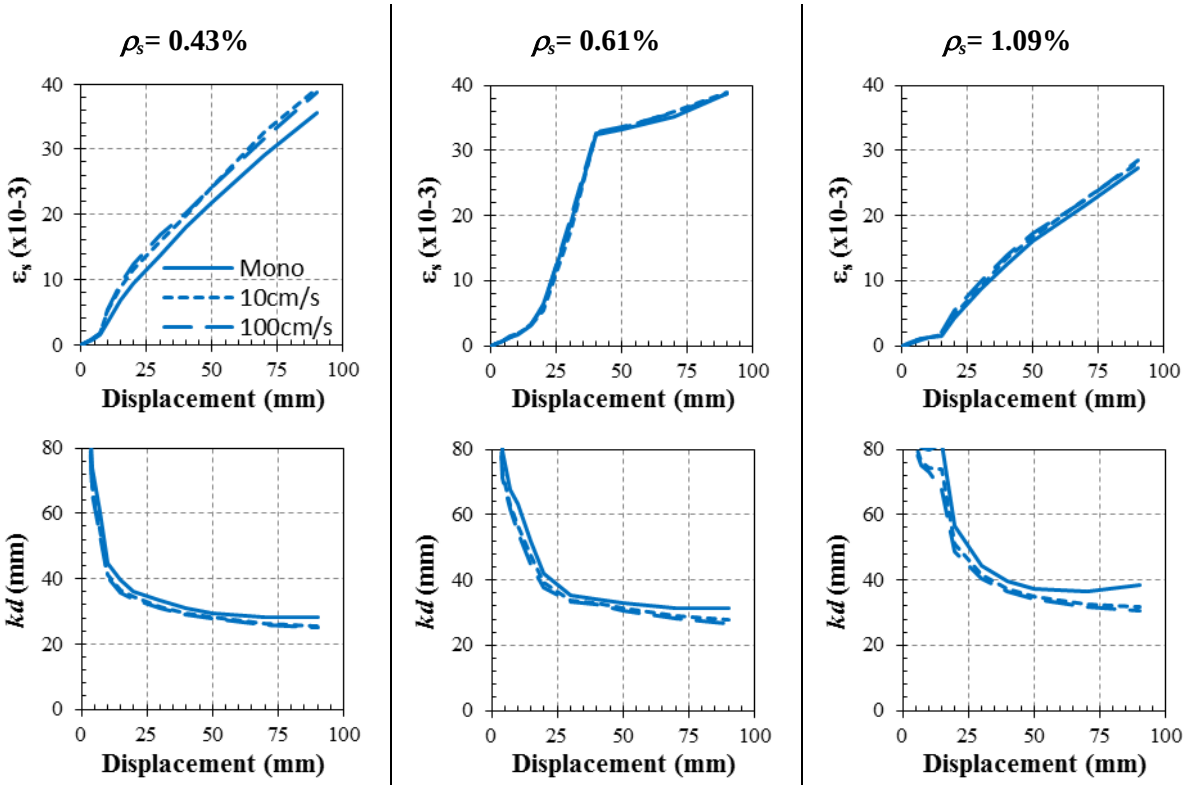

Figure 12. Steel strains and neutral axis depth from FE analyses varying the longitudinal reinforcement content and rate of loading. For all simulations, f'_c of 33MPa and f_y of 320MPa were used.

4 SUMMARY AND CONCLUDING REMARKS

This paper presents the qualitative framework of the ongoing research aiming at investigating the residual fatigue life of reinforced concrete frames at a component (or plastic hinge) level. Analytical and numerical work (and experimental tests at a later stage) is under development within this research program following the aforementioned framework.

Preliminary results of experimental and numerical investigations on well-designed reinforced concrete beam-to-column joints are also presented. The aim of such investigations is to identify and understand qualitatively and quantitatively the effect of parameters such as bond deterioration, steel and concrete material properties, as well as the amount of longitudinal reinforcement, on the cracking pattern and nonlinear behaviour of reinforced concrete plastic hinges.

Parametric analyses under monotonic loading have shown a lower amount of cracks but with wider openings are expected to occur for larger f'_c and smaller ρ_s values. Moreover, it was observed that although the overall behaviour in terms of strength, stiffness and strain limits is not significantly affected by variations in f_t, it strongly affects the expected cracking pattern in the beam-column joints, the latter being more uniformly distributed (i.e., larger amount and smaller crack widths) for lower f_t values. Furthermore, the seismic residual shear strength of the beam-column joints was observed to be influenced also by f'_c irrespective of the f_y and ρ_s values.

At this stage of preliminary results strain rate effects does not seem to play an important role on the cracking pattern. More investigation is under development to ascertain the above statement and define the relationship between key parameters and strain rates which could determine a change in the cracking pattern. In the cyclic response, the plastic strain at the most critical location decreases cycle after cycle (for the same drift demand), while the secant stiffness and hysteretic damping tend to become stable after a few cycles.

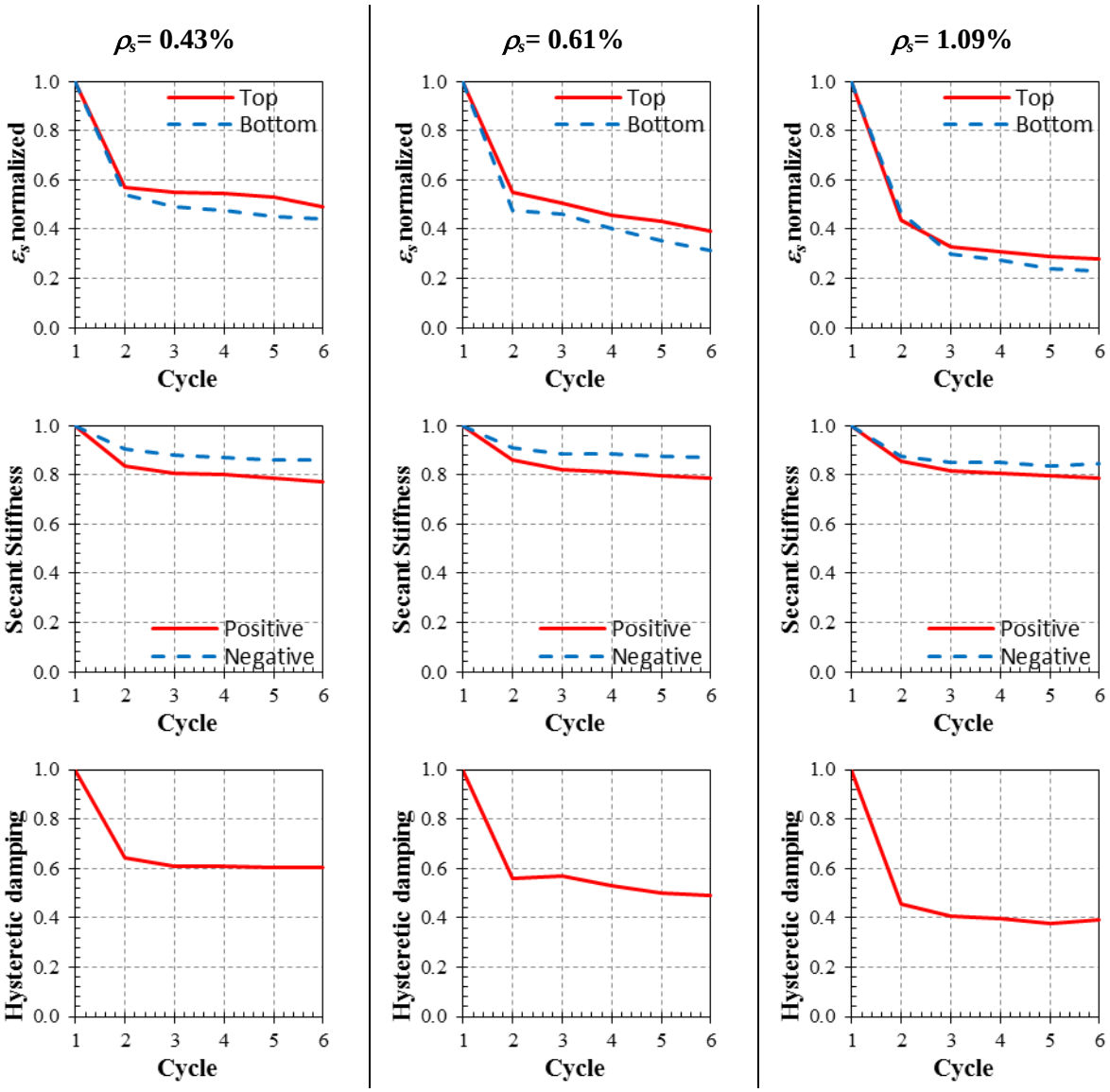

Figure 13. Cyclic story shear vs displacement response at 1.5% drift (a); cyclic variation of the strain at the longitudinal reinforcement (b); normalised secant stiffness (c); hysteretic damping (d); and snapshot at the end of the 6th cycle.

5 REFERENCES

Abdalla, J. A., Hawileh, R. A., & Abdelrahman, K. 2009. Energy-based prediction of low-cycle fatigue life of BS 460B and BS B500B steel bars, *Materials and Design*, Vol. 30:4405-4413.

Chung, L & Shah, S.P. 1989. Effect of loading rate on anchorage bond and beam-column joints, *ACI Structural Journal*, Vol. 86(2):132-142

Cuevas, A., & Pampanin, S. 2014. Accounting for residual capacity of reinforced concrete plastic hinges: current practice and proposed framework, *2014 New Zealand Society of Earthquake Engineering Conference,* Auckland, New Zealand.

Cuevas, A., Akguzel, U., Ožbotl, J. & Pampanin, S. 2014. Preliminary numerical investigation on the seismic residual capacity of reinforce concrete plastic hinges, *Second European Conference on Earthquake Engineering and Seismology*, Istanbul, Turkey

Eligehausen, R., Genesio, G., Ozbolt, J., & Pampanin, S. 2009. 3D analysis of seismic response of RC beam-column exterior joints before and after retrofit, *Concrete Repair, Rehabilitation and Retrofitting II*, 1141-1147.

Hawileh, R., Rahman, A. & Tabatabai, H. 2010. Evaluation of the low-cycle fatigue life in ASTM A706 and A615 grade 60 steel reinforcing bars, *Journal of Materials in Civil Engineering*, Vol. 22:65-76.

Henry, R.S. 2013. Assessment of the minimum vertical reinforcement limits for RC walls, *2013 New Zealand Society of Earthquake Engineering Conference*, Wellington, New Zealand.

Kunnath, S.K., El-Bahy, A., Taylor, A.W. & Stone, W.C. 1997. Cumulative seismic damage of reinforced concrete bridge piers, *National Institute of Standards and Technology*, NISTIR 6075.

Lettow, S. 2006. Ein Verbundelement für nichtlineare Finite Elemente Analysen – Anwendung auf Übergreifungsstöße (A bond element for nonlinear finite element analysis – Applied on splices), *PhD Dissertation, IWB, Universität Stuttgart, Germany (in German)*.

Maeda, M., Nakano, Y. & Lee, K.S. 2012. Post-earthquake damage evaluation for R/C buildings based on residual seismic capacity. *Proceedings of the 13th World Conference on Earthquake Engineering*, Vancouver, Canada.

Mander, J.B. & Cheng, C.T. 1999. Replaceable hinge detailing for bridge columns, *ACI Symposium Publications*, SP-187:185-204.

Mander, J.B. & Rodgers, G.W. 2013. Cyclic fatigue demands on structures subjected to the 2010-2011 Canterbury earthquake sequence, *2013 New Zealand Society of Earthquake Engineering Conference*, Wellington, New Zealand.

Mander, J.B., Panthaki, F.D. & Kasalanati, A. 1994. Low-cycle fatigue behaviour of reinforcing steel, *Journal of Materials in Civil Engineering*, Vol. 6(4):453-468.

Mendes, L.A.M, & Castro, L.M.S.S. 2014. A simplified reinforcing steel model suitable for cyclic loading including ultra-low-cycle fatigue effects, *Engineering Structures*, Vol. 28:155-164.

Ožbolt J, Yijun L, & Kozar I. 2001. Microplane model for concrete with relaxed kinematic constraint, *International Journal of Solids and Structures*, Vol. 38:2638-711.

Ožbolt J, Sharma A & Reinhardt H. 2011. Dynamic fracture of concrete – compact tension specimen, *International Journal of Solids and Structures*, Vol. 48:1534-1543.

Ožbolt J & Sharma A. 2011. Numerical simulation of reinforced concrete beams with different shear reinforcements under dynamic impact loads, *International Journal of Impact Engineering*, Vol. 38:940-950.

Pampanin, S. 2012. Reality-check and renewed challenges in earthquake engineering: implementing low-damage structural systems – from theory to practice, *Fifteenth World Conference in Earthquake Engineering*, Lisbon, Portugal.

Polese, M., Di Ludovico, M., Prota, A. & Manfredi, G. 2012. Residual capacity of earthquake damaged buildings. *Proceedings of the 15th World Conference on Earthquake Engineering*, Lisbon, Portugal.

Priestley, M.N.J., Calvi, G.M. & Kowalsky, M.J. 2007. *Displacement-based seismic design of structures*, IUSS Press, Pavia, Italy.

SESOC. 2011. *Preliminary observations from Christchurch earthquakes*, Structural Engineering Society, New Zealand.